DOI: 10.1002/chem.201200363

Solvent-Catalyzed Ring–Chain–Ring Tautomerization in Axially Chiral Compounds

Asli Yildirim,[a] Fethiye Aylin Sungur Konuklar,[b] Saron Catak,*[c] Veronique Van Speybroeck,[c] Michel Waroquier,[c] Ilknur Dogan,[a] and Viktorya Aviyente*[a]

Abstract: The mechanism of ring–chain–ring tautomerization and the prominent effect of the solvent environment have been computationally investigated in an effort to explain the enantiomeric interconversion observed in 2-oxazolidinone derivatives, heterocyclic analogues of biphenyl atropisomers, which were isolated as single stable enantiomers and have the potential to be used as axially chiral catalysts. This study has shed light on the identity of the intermediate species involved in the ring–chain–ring tautomerization process as well as the catalytic effect of polar protic solvents. These mechanistic details will prove very useful in predicting and understanding ring–chain tautomeric equilibria in similar heterocyclic systems and will further enable experimentalists to devise appropriate experimental conditions in which axially chiral catalysts remain stable as single enantiomers.

Keywords: biaryls · chirality · density functional calculations · microsolvation · tautomerization

Introduction

Ring–chain–ring tautomerization is a process that involves a proton-shift-assisted ring opening followed by a ring closure and is a significant step in the organic synthesis of five- and six-membered 1,3-heterocycles containing oxygen, nitrogen, or sulfur atoms.[1] In the past decade, ring–chain tautomeric equilibria have been studied for 1,3-X,N-heterocyclic systems (X = S, O) with great interest[2] and have also attracted attention in physical and medicinal chemistry.[3]

Recent studies have shown that ring–chain–ring tautomerization is a key pathway for the synthesis of various important compounds. Thiazolidinyloxazolidines and spirothiazolidines, which are analogues of bis-oxazolidines notably used as chiral catalysts[4] and anticancer[5] and neuroprotective agents,[6] have been obtained from the ring–chain tautomerization of mercaptomethyl bis-oxazolidine.[7] Furthermore, this process has also been observed in the conversion of bicyclo[4.2.0]octane derivatives into trisubstituted enamines.[8] Two recent studies have proved the existence of ring–chain tautomerization in simplified analogues of isoniazid-NAD(P) adducts, which are known for their prominent activity against Mycobacterium tuberculosis,[9] and in 2-ferrocenyl-2,4-dihydro-1*H*-3,1-benzoxazines.[10]

The ring–chain tautomerization process has been shown to occur in heterocyclic compounds, such as in a novel 1,3-imidazolidine containing a vinyloxy group[2a] as well as in pyrazolidine, pyridazine, and oxazolidine derivatives, which are of particular interest in this study.[11,12]

Compounds comprising the oxazolidine ring, which are also the subject of this study, have been introduced as drugs for the treatment of insulin resistance, hyperglycemia, and some lipid disorders.[13–15] The chemical importance of these compounds is not limited to medicinal chemistry, oxazolidine derivatives have also been used as directing groups in asymmetric synthesis.[16,17]

N-(*o*-Aryl)-5,5-dimethyl-2,4-oxazolidinedione derivatives **1** and *N*-(*o*-aryl)rhodanines (X=S) and 2-oxazolidinethiones (X=O) **2** (Scheme 1) are heterocyclic compounds that have a chiral axis enabling the formation of thermally interconvertible enantiomers by hindered rotation around the N–C_{aryl} bond.[18–21] The synthesis of atropisomeric compounds, molecules that bear a chiral axis rather than a stereogenic atom and have barriers to rotation that are high enough to allow the isolation of enantiopure species, is currently of particular interest in many studies. The best-known atropisomeric systems are biaryl compounds with *ortho* substituents that hinder rotation and prevent racemization. Atropisomers are used as effective chiral catalysts enabling the transmission of chiral information during reactions.[22] Recent advances in this field include an effective method for the enantio-

[a] A. Yildirim, Prof. Dr. I. Dogan, Prof. Dr. V. Aviyente
Department of Chemistry, Boğaziçi University
Bebek, Istanbul, 34342 (Turkey)
Fax: (+90) 212-287-24-67
E-mail: aviye@boun.edu.tr

[b] Prof. Dr. F. A. S. Konuklar
Informatics Institute, Istanbul Technical University
Maslak, Istanbul, 34469 (Turkey)

[c] Dr. S. Catak, Prof. Dr. V. Van Speybroeck, Prof. Dr. M. Waroquier
Center for Molecular Modeling, Ghent University
Technologie Park 903, 9052 Zwijnaarde (Belgium)
Fax: (+32) 9-264-66-97
E-mail: saron.catak@ugent.be

Supporting information for this article is available on the WWW under http://dx.doi.org/10.1002/chem.201200363.

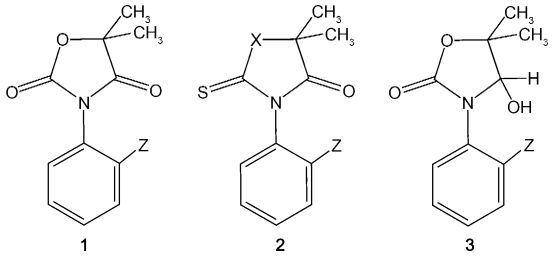

Scheme 1. Structures of *N*-(*o*-aryl)-5,5-dimethyl-2,4-oxazolidinedione **1**, *N*-(*o*-aryl)-5,5-dimethylrhodanine (X=S) and 2-oxazolidinethiones (X=O) **2**, and *N*-(*o*-aryl)-4-hydroxy-5,5-dimethyl-2-oxazolidinone derivatives **3** (Z=F, Cl, Br, I or Me).

selective construction of biaryl compounds devised by Thomson and co-workers.[23] Furthermore, Miller and co-workers have described a dynamic kinetic resolution of biaryl atropisomers by peptide catalysis[24] and Cozzi et al. have applied organocatalysis to atroposelective reactions.[25] Moreover, in a combined experimental and computational study, atropisomerism has been created by introducing *ortho*-substituted aryl groups into peptoid backbones.[26] Nevertheless, Roussel et al. have claimed that internal rotation does not account for the trend in the activation barriers for some 2-pyrimidinethione derivatives and have suggested a ring-opening–ring-closure mechanism rather than hindered rotation around the N–C_{aryl} bond.[27]

In a comprehensive study, Demir-Ordu and Dogan investigated the interconversion between the *SM* and *RP* enantiomers of *N*-(*o*-aryl)-4-hydroxy-5,5-dimethyl-2-oxazolidinone derivatives **3** (Scheme 1)[12] and proposed a racemization that occurs through a "ring–chain–ring tautomerization" mechanism.[12] To clarify the mechanism, the interconversion of the enantiomer in ethanol was followed by HPLC and the activation barrier for the interconversion of *SM* into *RP* was reported to be 25.3 kcal mol^{-1}.[12] The interconversion was suggested to occur via an acyclic aldehyde intermediate formed by ring–chain tautomerization. The aldehyde intermediate, although not observed on the NMR timescale in $CDCl_3$, was treated with benzylamine in toluene and trapped in the form of an imine. The product was identified as having a cyclic aminal structure formed by attack of the NH group on the formed imine. Thus, the presence of the acyclic aldehyde intermediate was verified indirectly by ^{1}H and ^{13}C NMR characterization of the cyclic aminal product formed after its treatment with benzylamine in toluene.[12] 2-Oxazolidinone derivatives **3** are heterocyclic analogues of biphenyl atropisomers and have been found to be resolvable by HPLC on a chiral column. These separated enantiomers have the potential to be used as axially chiral catalysts.[12] Thus, it is imperative to gain more insight into their modes of racemization in order to be able to establish the conditions in which they remain stable as single enantiomers.

It is difficult to assess the mechanism that governs the racemization process on a purely experimental basis. However, theoretical methods have the potential to identify various factors and hence a computational investigation of the mechanism of ring–chain–ring tautomerization in *N*-(*o*-tolyl)-4-hydroxy-5,5-dimethyl-2-oxazolidinone (**3**, Z= methyl) has been carried out by means of DFT calculations to gain an in-depth understanding of the mechanism involved (Scheme 2).

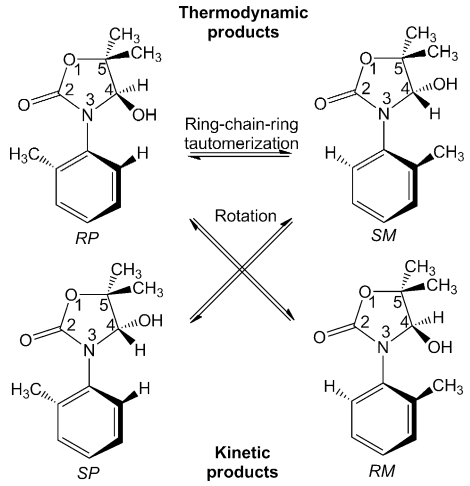

Scheme 2. Rotation and ring–chain–ring tautomerization of 2-oxazolidinone **3**.

Results and Discussion

Rotation around the N–C_{aryl} bond: The reduction of **1** with $NaBH_4$ at C4 was expected to lead to four stereoisomers (*RP*, *SM*, *SP*, and *RM*) of **3** as a result of the new chiral center at C4 (Scheme 2). The kinetic products (*SP* and *RM*) that form in accord with the Felkin–Anh model,[28] that is, by hydride attack of the *ortho*-phenyl substituent from the *anti* direction, were converted into the thermodynamic products (*RP* and *SM*) by a fast rotation around the N–C_{aryl} bond. As a result, the hydroxy group at C4 and the *ortho*-phenyl substituent are antiplanar with respect to each other (*RP* and *SM*) (Scheme 2).[12]

Initially, the rotation around the N–C_{aryl} bond of **3** was studied. The ground-state configuration of *RP* and the corresponding rotational transition state between *RP* and *RM* are displayed in Figure 1. The rotational transition state (**TS-Rot**) has a dihedral angle of $\theta_{a\text{-}b\text{-}c\text{-}d}=180.3°$, the four atoms being planar. In the ground state of *RP*, $\theta=71.3°$. In the kinetically favored product (*RM*, $\theta=-72.7°$) the methyl and hydroxy groups face each other and are in a sterically unfavorable orientation, thereby increasing its energy. We were also able to localize a second rotational transition state that is also quasiplanar ($\theta=-2.8°$), but it was found to be higher in energy (by 3.8 kcal mol^{-1}, see the Supporting Information) due to the lack of favorable interactions between the hydroxy group at C4 and the methyl hydrogen atoms of the *ortho*-phenyl substituent.

In *RP*, the lone pair of the hydroxy oxygen has a favorable interaction with the methyl hydrogen atoms at C5. In

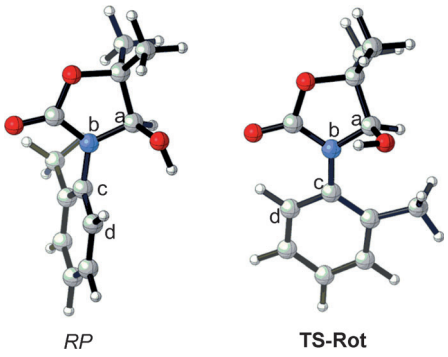

Figure 1. *RP* (lowest ground state) and **TS-Rot** (rotational transition state) of 2-oxazolidinone **3** determined by DFT calculations at the B3LYP/6-31+G(d,p) level of theory.

TS-Rot, the methyl hydrogen atoms at the *ortho* position of the phenyl ring repel the hydroxy unit at C4, however, a favorable hydrogen bond between the hydroxy group and the nitrogen is present (Figure 1). The same situation holds for the *SM*/*SP* pair.

The results of the theoretical calculations on the rotation are shown in Table 1 (rotational free-energy profiles can be found in the Supporting Information). The experimentally

Table 1. Rotational free-energy barriers (298.15 K) determined at various levels of theory for 2-oxazolidinone **3**.[a–c]

Method	$\Delta G^{\neq}_{\text{Rotation}}$ [kcal mol^{-1}]	
	RM/*RP* rotation	*SM*/*SP* rotation
B3LYP	9.4 [10.4]	9.6 [11.1]
BMK	9.2 [10.4]	9.3 [10.9]
M06-2X	9.0 [10.1]	9.2 [10.7]
MPWB1K	9.0 [10.1]	9.1 [10.7]
MP2	9.2	9.6
SCS-MP2	9.9	10.3

[a] Basis set: 6-311+G(3df,2p). [b] Values in brackets were obtained from CPCM calculations with the same basis set. [c] Geometry optimizations: B3LYP/6-31+G(d,p).

hypothesized fast rotation is validated by the calculated low rotational barrier (ca. 10 kcal mol^{-1}), which leads to the formation of the thermodynamic products *SM* and *RP*. However, these rotational barriers do not correspond to the experimentally determined barrier to tautomerization (25.3 kcal mol^{-1}).[12] Moreover, rotation around the N–C_{aryl} bond cannot account for the experimentally observed interconversion of *SM* into *RP*.

Ring–chain–ring tautomerization: After the formation of the thermodynamic products, heating of the resolved single *RP* enantiomer to 323 K led to conversion into its counterpart, *SM*. This was proposed to occur by ring opening of the heterocyclic ring followed by reclosure because the interconversion between *RP* and *SM* cannot be achieved by a rotational mechanism. The ring–chain–ring tautomerization mechanism for the conversion of *RP* into *SM* proceeds by

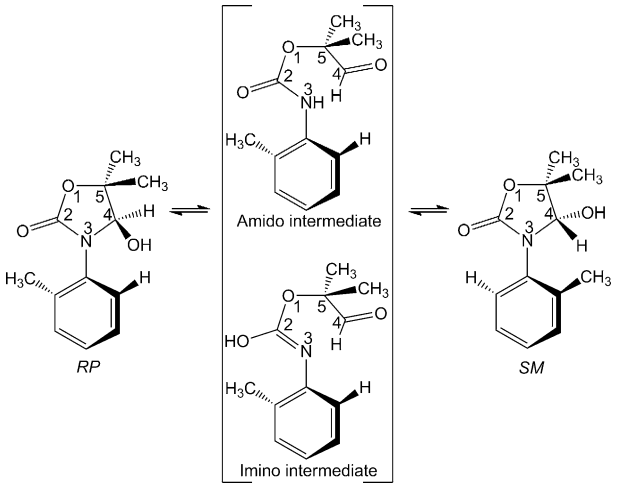

Scheme 3. Ring-chain-ring tautomerization of 2-oxazolidinone **3** via an amido or imino acyclic intermediate.[12]

N3–C4 bond cleavage leading to the formation of an acyclic aldehyde intermediate (Scheme 3).[12] The ring subsequently closes by *Si* or *Re* face attack of the nitrogen leading to the formation of the corresponding enantiomer.

The interconversion of *RP* into *SM* by the ring–chain–ring tautomerization mechanism could, in principle, occur via both an amido and/or imino intermediate (Scheme 3). Herein we investigate by theoretical calculations the mechanistic details of the tautomerization pathway of 2-oxazolidinone **3** to elucidate whether the amido or imino intermediate occurs and whether both pathways are possible.

As the tautomerization takes place in ethanol, we investigated the effect of the environment by calculating the reaction profiles with and without the assistance of explicit solvent (ethanol) molecules. Bulk solvation effects were also taken into account.

Microsolvation, solvating with explicit solvent molecules, has extensively been used in modeling reaction mechanisms in which the solvent plays a particular stabilizing role.[29] The use of solvent molecules in the assistance of the proton transfer steps, as in the case here, has proven to be crucial because the solvent serves as the proton conduit.[30] Furthermore, several studies have shown that reactions involving the carbonyl functionality, such as peptidic amides, first interconvert into their more reactive tautomeric counterparts; these tautomerization steps were also shown to be facilitated by polar protic solvents.[30d,f,g,i]

First, the amido mechanism (Scheme 3) was investigated without the assistance of ethanol molecules. The potential energy surface for this pathway, which illustrates the interconversion of *RP* into *SM*, is displayed in Figure 2. The ground-state *RP* yields the acyclic **Amido intermediate 1** via ***RP* TS Amido No EtOH**, the bond cleavage having a barrier of 48.5 kcal mol^{-1}; this intermediate undergoes rotation around the N–C_{aryl} bond to give **Amido intermediate 2**. In this step the *P* configuration of the aryl ring changes into the *M* configuration. Then rotation around the C4–C5 bond

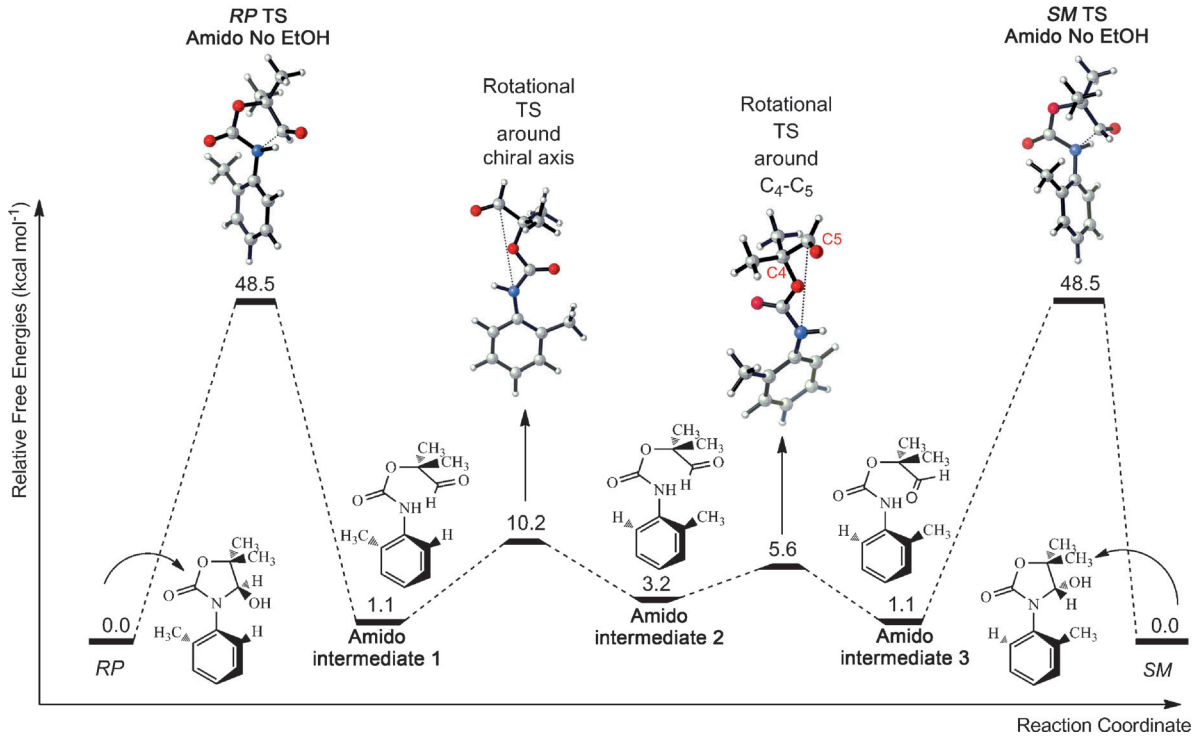

Figure 2. Potential energy surface for the ring–chain–ring tautomerization of *RP* via an acyclic amido intermediate (B3LYP/6-311+G(3df,2p)//B3LYP/6-31+G(d,p)).

occurs to yield **Amido intermediate 3** and the *R* configuration of the stereocenter in the reactant is ready to yield the *S* configuration in the product. Note that all amido intermediates are plausible conformers of each other. Finally, ring closure occurs to yield the *SM* enantiomer. The two ground states (*RP* and *SM*) and the ring-opening and ring-closure transition states (***RP* TS Amido No EtOH** and ***SM* TS Amido No EtOH**, respectively) are mirror images of each other (Figure 2).

The two rotational barriers are significantly lower than that of the first step in which bond rupture occurs, hence the ring-opening step for the *RP* enantiomer is identified as the rate-determining step in the ring–chain–ring tautomerization process. However, because the barrier for this step is unrealistically high, the effect of solvent assistance on this step has been explored. The transition-state structures for the aforementioned ring-opening step are shown with and without explicit (ethanol) molecules in Figure 3. Visual inspection of the transition-state structures clearly shows that the ring-opening step is prone to assistance by solvent bridges, in line with the Grotthus mechanism,[31] which suggests proton transport occurs through molecular wires. The barriers for ring–chain–ring tautomerization corresponding to C4–N3 bond rupture are summarized in Table 2 at various levels of theory.

The assistance of protic ethanol molecules lowers the barrier on average by about 10 kcal mol^{-1}, but still the barriers remain too high by at least 10 kcal mol^{-1} compared with values determined experimentally (25.3 kcal mol^{-1}). There-

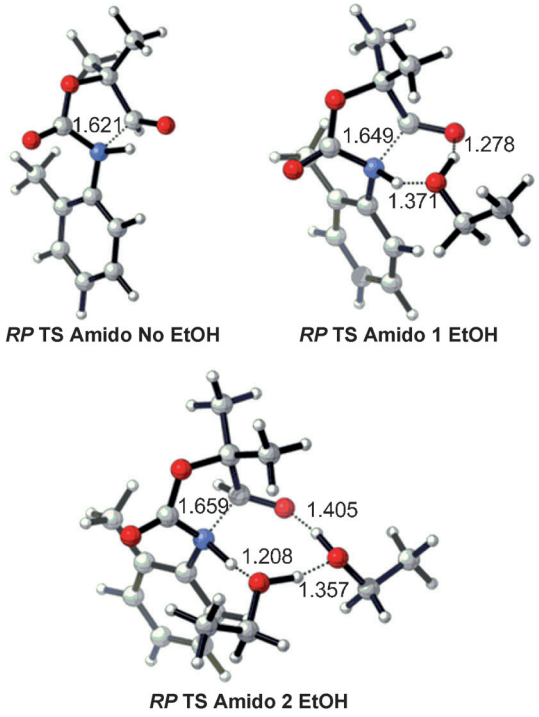

Figure 3. Optimized transition-state geometries for ring–chain–ring tautomerization via the "amido" acyclic intermediate (B3LYP/6-31+G(d,p)). Critical distances given in Å.

Table 2. Free-energy barriers (323 K) at various levels of theory for the ring–chain–ring tautomerization of 2-oxazolidinone **3** via the "amido" intermediate.[a–d]

Method	$\Delta G^{\neq}_{\text{Ring-opening}}$ [kcal mol^{-1}]		
	Amido No EtOH	**Amido 1 EtOH**	**Amido 2 EtOH**
B3LYP	48.5 [47.8]	37.3 [36.6]	39.7 [37.7]
BMK	50.8 [50.0]	40.3 [39.5]	41.4 [39.3]
M06-2X	51.4 [50.7]	37.5 [36.7]	36.0 [33.9]
MPWB1K	53.1 [52.3]	42.1 [41.3]	43.8 [41.7]
MP2	48.5	35.8	35.2
SCS-MP2	50.3	39.3	39.8
B3LYP-PCM opt.[e]	50.6 [49.9]	37.9 [37.1]	40.8 [38.9]

[a] Basis set: 6-311+G(3df,2p). [b] Values in brackets obtained from CPCM calculations with the same basis set. [c] Geometry optimizations: B3LYP/6-31+G(d,p). [d] Experimental value: 25.3 kcal mol^{-1} at 323 K. [e] These energies refer to PCM optimized geometries with B3LYP/6-31+G(d,p).

Table 3. Free-energy barriers (323 K) at various levels of theory for the ring–chain–ring tautomerization of 2-oxazolidinone **3** via the "imino" intermediate.[a–d]

Method	$\Delta G^{\neq}_{\text{Ring-opening}}$ [kcal mol^{-1}]	
	Imino 1 EtOH	**Imino 2 EtOH**
B3LYP	35.5 [36.3]	27.0 [26.8]
BMK	38.3 [39.0]	30.0 [29.7]
M06-2X	35.5 [36.1]	27.0 [26.6]
MPWB1K	38.2 [38.9]	31.0 [30.6]
MP2	35.6	27.5
SCS-MP2	39.2	30.8
B3LYP-PCM opt.[e]	36.7 [36.7]	29.7 [27.4]

[a] Basis set: 6-311+G(3df,2p). [b] Values in brackets obtained from CPCM calculations with the same basis set. [c] Geometry optimizations: B3LYP/6-31+G(d,p). [d] Experimental value: 25.3 kcal mol^{-1} at 323 K. [e] These energies refer to PCM optimized geometries with B3LYP/6-31+G(d,p).

fore the interconversion of *RP* into *SM* was also explored via the "imino" form of the aldehyde intermediate, as shown in Scheme 3. In the case of the imino intermediate, it was impossible to locate the transition state without solvent assistance. This can easily be rationalized by inspecting some critical distances between pairs of atoms involved in the reaction coordinate. In this case the distance between the carbonyl oxygen at the C2 position and the hydroxy group at C4 is too large (3.833 Å) to allow direct proton transfer between these two centers. In the imino mechanism, one (***RP* TS Imino 1 EtOH**) or two ethanol molecules (***RP* TS Imino 2 EtOH)** act as a bridge in the transfer of a proton from the hydroxy group at C4 to the carbonyl oxygen at C2 (Figure 4). Both the proton transfer and the

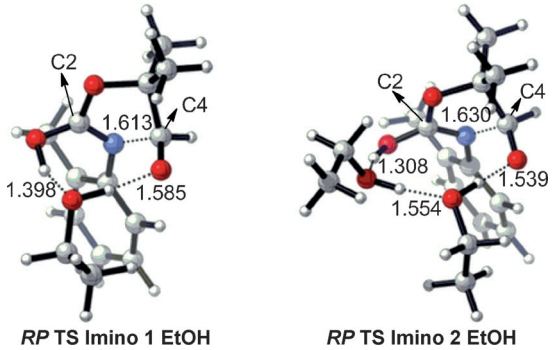

Figure 4. Optimized transition-state geometries for ring–chain–ring tautomerization via the "imino" acyclic intermediate (B3LYP/6-31+G(d,p)). Critical distances given in Å.

C4–N3 bond cleavage occur simultaneously leading to the formation of the acyclic imino structure. Subsequently, with the attack of N3 from the opposite side, the *SM* isomer forms. The assistance of two ethanol molecules in the formation of an acyclic imino intermediate further lowers the barrier to ring opening (Table 3). At all levels of theory, the activation barrier for ring opening in the presence of two ethanol molecules becomes remarkably close to the experimental value.

Based on the perfect agreement between the theoretically determined free-energy barriers (imino mechanism 27 kcal mol^{-1}) and the experimental value (25.3 kcal mol^{-1}), it can be concluded that the ring–chain–ring tautomerization occurs by the imino mechanism. An overview of the entire pathway for the *RP*/*SM* interconversion by the "solvent-assisted imino mechanism" and the corresponding potential energy surface is shown in Figure 5. In short, the ground-state *RP* (***RP* 2 EtOH**) undergoes ring opening to yield the acyclic **Imino intermediate 1**, which then gives **Imino intermediate 3** by overcoming two rotational steps, as previously shown in Figure 2. Finally, the **Imino intermediate 3** converts into the *SM* (***SM* 2 EtOH**) by ring closure. Compared with the "non-assisted amido mechanism" (Figure 2), the rotational barriers for the imino mechanism with two ethanol molecules were found to be slightly higher, however, it is again clearly seen that the rate-determining step for the interconversion of *RP* into *SM* is the ring-opening step for the *RP* enantiomer, as expected.

The amido and imino forms of the acyclic intermediate, which are formed by the ring opening of the *RP* enantiomer, are shown in Figure 6 with two solvating ethanol molecules. The main difference between these intermediates is the C2 atom and its substituents. In the **Amido intermediate 1** there is a carbonyl group at the C2 position, whereas in the **Imino intermediate 1** this center is in its corresponding tautomeric form. The amido intermediate is the result of proton transfer between the hydrogen atom at N3 and the carbonyl group at C4; the imino intermediate is the outcome of proton transfer between the OH group at C2 and the carbonyl group at C4.

Solvent molecules are aligned to assist proton transfer. The distance between N3 and C4 is 2.796 Å in the amido intermediate, whereas it is 2.532 Å in the imino intermediate. Although the barriers leading to the imino intermediate are lower, the intermediate itself is slightly higher in energy than the amido intermediate (ca. 4 kcal mol^{-1} for solvated systems, see the Supporting Information).

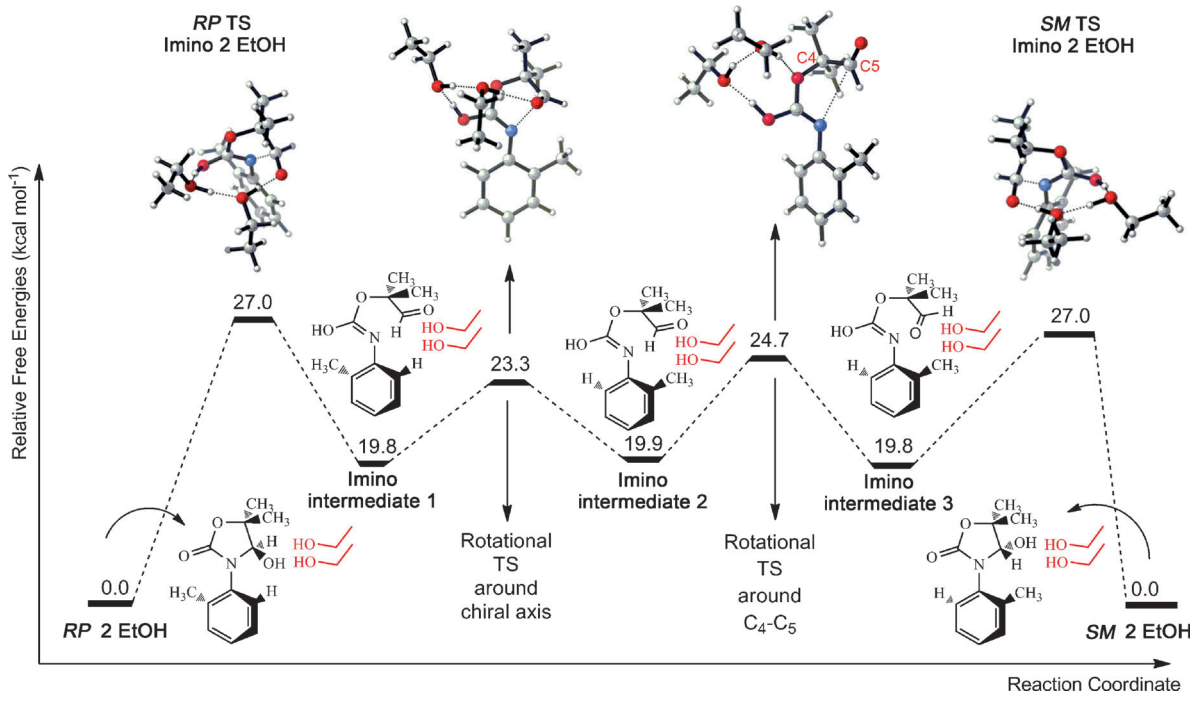

Figure 5. Potential energy surface for the ring–chain–ring tautomerism of **RP 2 EtOH** via the imino intermediate (B3LYP/6-311+G(3df,2p)//B3LYP/6-31+G(d,p)).

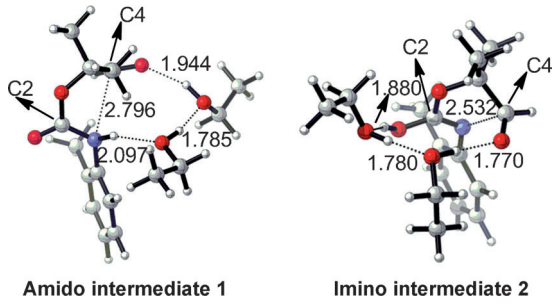

Figure 6. Amido and imino acyclic intermediate structures of 2-oxazolidinone **3** with two ethanol molecules (B3LYP/6-31+G(d,p)). Critical distances given in Å.

Conclusion

In this paper, the enantiomeric interconversion observed for 2-oxazolidinone derivatives **3**, heterocyclic analogues of biphenyl atropisomers with potential to be used as axially chiral catalysts, has been theoretically assessed; the mechanism of their interconversion as well as the environmental factors that contribute to their racemization have been thoroughly elucidated.

This study has shown that the *SM* and *RP* enantiomeric pairs of *N*-(*o*-tolyl)-4-hydroxy-5,5-dimethyl-2-oxazolidinone (**3**) interconvert through a ring–chain–ring tautomerization mechanism. An acyclic aldehyde intermediate was previously suggested, although not experimentally isolated; this study has revealed that the ring–chain–ring tautomerization occurs via an "imino intermediate" rather than an "amido intermediate".

Solvent effects were found to be essential in the reaction mechanism because proton-hopping is facilitated by the presence of assisting ethanol molecules, in line with the proton transport suggested for hydrogen-bonded solvents in the Grotthus mechanism.[31] Although the kinetic functionals BMK[32] and MPWB1K[33] slightly overestimated the ring-opening barrier, M06-2X,[34] known to perform well in organic systems with dispersive effects,[29e,35] showed results that are consistent with the experimental findings.

In summary, this theoretical study has shed light on the conditions in which 2-oxazolidinone derivatives **3**, which are potential chiral catalysts, remain stable as single enantiomers. The role of solvent is crucial in the racemization process. Hence, the use of aprotic solvents will likely suppress racemization. The results of this work will prove very useful for similar heterocyclic analogues of biphenyl atropisomers that are used as axially chiral catalysts.

Computational Section

Geometry optimizations and frequency calculations at the B3LYP/6-31+G(d,p)[36] level of theory were performed by using the Gaussian 03 and 09 program packages.[37] The intrinsic reaction coordinate (IRC)[38] for the ring–chain–ring tautomerization path was traced to connect the transition-state structures and the corresponding reactants and products. Zero-point energies and thermal corrections were obtained from vibrational frequencies, which were also used to confirm the nature of the stationary points. Energy values for the rotational barriers include thermal free-energy corrections at 298.15 K and 1 atm, whereas energy values for

the ring–chain–ring tautomerization mechanism were calculated at 323 K to comply with the experimental conditions. The effect of a polar environment was taken into account through single-point calculations by the use of the self-consistent reaction field (SCRF)[39] theory, utilizing the conductorlike polarizable continuum (CPCM)[40] model in ethanol. The UFF cavity model[41] in Gaussian 09 was used. Energy values for solvent calculations include thermal free-energy corrections taken from gas-phase optimizations. Single-point energy calculations were performed for all structures at the B3LYP,[36] BMK,[32] MPWB1K,[33] MP2,[42] SCS-MP2,[43] and M06-2X[34] levels by using the 6-311+G(3df,2p) basis set on B3LYP/6-31+G(d,p) optimized structures. At each level of theory, the free energies include the thermal free-energy corrections obtained from gas-phase calculations at the B3LYP/6-31+G(d,p) level.

Acknowledgements

The computational resources used in this work was provided by Stevin Supercomputer Infrastructure Ghent University (Belgium), the Hercules Foundation and the Flemish Government-Department EWI, and the National Center for High Performance Computing of Turkey (UHEM) (grant no. 11042010) and project DPT-2009K120520. The UGent authorsthank the FWO (Fonds voor Wetenschappelijk Onderzoek–Vlaanderen, Fund for Scientific Research e Flanders), the research board of Ghent University for the bilateral project Ghent–Istanbul and the IAP-BELSPO project in the frame of IAP 6/27 for financial support of this research.

[1] J. B. Lambert, G. T. Wang, D. E. Huseland, L. C. Takiff, *J. Org. Chem.* **1987**, *52*, 68–71.
[2] a) N. A. Keiko, N. V. Vchislo, L. G. Stepanova, L. I. Larina, Y. A. Chuvashev, E. A. Funtikova, *Chem. Heterocycl. Compd.* **2008**, *44*, 1466–1471; b) L. Lázár, F. Fulöp, *Eur. J. Org. Chem.* **2003**, 3025–3042.
[3] I. Szatmári, T. A. Martinek, L. Lazar, A. Koch, E. Kleinpeter, K. Neuvonen, F. Fulöp, *J. Org. Chem.* **2004**, *69*, 3645–3653.
[4] S. L. Shi, L. W. Xu, K. Oisaki, M. Kanai, M. Shibasaki, *J. Am. Chem. Soc.* **2010**, *132*, 6638–6639.
[5] Y. Shintani, T. Tanaka, Y. Nozaki, *Cancer Chemother. Pharmacol.* **1997**, *40*, 513–520.
[6] K. E. Desino, S. Ansar, G. I. Georg, R. H. Himes, M. L. Michaelis, D. Powell, E. A. Reiff, H. Telikepalli, K. L. Audus, *J. Med. Chem.* **2009**, *52*, 7537–7543.
[7] C. Saiz, P. Wipf, G. Mahler, *J. Org. Chem.* **2011**, *76*, 5738–5746.
[8] V. Y. Korotaev, A. Y. Barkov, P. A. Slepukhin, M. I. Kodess, V. Y. Sosnovskikh, *Tetrahedron Lett.* **2011**, *52*, 3029–3032.
[9] T. Delaine, V. Bernardes-Genisson, J. Stigliani, H. Gornitzka, B. Meunier, J. Bernadou, *Eur. J. Org. Chem.* **2007**, 1624–1630.
[10] S. Pérez, C. Lopez, A. Caubet, A. Roig, E. Molins, *J. Org. Chem.* **2005**, *70*, 4857–4860.
[11] J. Sinkkonen, V. Ovcharenko, K. N. Zelenin, I. P. Bezhan, B. A. Chakchir, F. Al-Assar, K. Pihlaja, *Eur. J. Org. Chem.* **2002**, 3447–3454.
[12] Ö. Demir-Ordu, I. Dogan, *Chirality* **2010**, *22*, 641–654.
[13] Y. Momose, T. Maekawa, T. Yamano, M. Kawada, H. Odaka, H. Ikeda, T. Sohda, *J. Med. Chem.* **2002**, *45*, 1518–1534.
[14] B. B. Lohray, V. Bhushan, *Curr. Med. Chem.* **2004**, *11*, 2467–2503.
[15] I. Jin, N. Morales-Ramos, P. Eidam, J. Mecom, Y. Li, C. Brooks, M. Hilfiker, D. Zhang, N. Wang, D. Shi, P. Tseng, K. Wheless, B. Budzik, K. Evans, J. Jaworski, J. Jugus, L. Leon, C. Wu, M. Pullen, B. Karamshi, P. Rao, E. Ward, N. Laping, C. Evans, C. Leach, D. Holt, X. Su, D. Morrow, H. Fries, K. Thorneloe, R. Edwards, *ACS Med. Chem. Lett.* **2010**, *1*, 316–320.
[16] G. Q. Lin, Y. M. Li, A. S. C. Chan, *Principles and Applications of Asymmetric Synthesis*, Wiley, New York, **2001**, p. 135–188.
[17] R. A. Aitken, S. N. Kilenyi, *Asymmetric Synthesis*, Blackie Academic Professional, London, **1992**, p. 83–140.
[18] Y. Aydeniz, F. Oğuz, A. Yaman, F. A. Konuklar (Sungur), I. Doğan, V. Aviyente, A. K. Klein, *Org. Biomol. Chem.* **2004**, *2*, 2426–2436.
[19] Ö. Demir Ordu, I. Dogan, *Tetrahedron: Asymmetry* **2004**, *15*, 925–933.
[20] E. M. Yilmaz, I. Dogan, *Tetrahedron: Asymmetry* **2008**, *19*, 2184–2191.
[21] Ö. Demir-Ordu, E. M. Yilmaz, I. Dogan, *Tetrahedron: Asymmetry* **2005**, *16*, 3752–3761.
[22] a) J. Clayden, W. J. Moran, P. J. Edwards, S. R. LaPlante, *Angew. Chem.* **2009**, *121*, 6516–6520; *Angew. Chem. Int. Ed.* **2009**, *48*, 6398–6401.
[23] F. Guo, L. C. Konkol, R. J. Thomson, *J. Am. Chem. Soc.* **2011**, *133*, 18–20.
[24] J. L. Gustafson, D. Lim, S. J. Miller, *Science* **2010**, *328*, 1251–1255.
[25] P. G. Cozzi, E. Emer, A. Gualandi, *Angew. Chem.* **2011**, *123*, 3931–3933; *Angew. Chem. Int. Ed.* **2011**, *50*, 3847–3849.
[26] B. Paul, G. L. Butterfoss, M. G. Boswell, P. D. Renfrew, F. G. Yeung, N. H. Shah, C. Wolf, R. Bonneau, K. Kirshenbaum, *J. Am. Chem. Soc.* **2011**, *133*, 10910–10919.
[27] C. Roussel, M. Adjimi, A. Chemlal, A. Djarfi, *J. Org. Chem.* **1988**, *53*, 5076–5080.
[28] J. Seyden-Penne, *Reductions by the Alumino- and Borohydrides in Organic Synthesis*, Wiley-VCH, Weinheim, **1997**, p. 45–51.
[29] For recent reports on microsolvation and selected applications of mixed explicit/implicit solvent models, see: a) J. R. Pliego, J. M. Riveros, *J. Phys. Chem. A* **2001**, *105*, 7241–7247; b) C. P. Kelly, C. J. Cramer, D. G. Truhlar, *J. Phys. Chem. A* **2006**, *110*, 2493–2499; c) E. F. da Silva, H. F. Svendsen, K. M. Merz, *J. Phys. Chem. A* **2009**, *113*, 6404–6409; d) L. Hermosilla, S. Catak, V. Van Speybroeck, M. Waroquier, J. Vandenbergh, F. Motmans, P. Adriaensens, L. Lutsen, T. Vanderzande, *Macromolecules* **2010**, *43*, 7424–7433; e) S. Catak, M. D'hooghe, N. De Kimpe, M. Waroquier, V. Van Speybroeck, *J. Org. Chem.* **2010**, *75*, 885–896; f) M. D'hooghe, S. Catak, S. Stanković, M. Waroquier, Y. Kim, H. J. Ha, V. Van Speybroeck, N. De Kimpe, *Eur. J. Org. Chem.* **2010**, 4920–4931; g) S. Catak, M. D'hooghe, T. Verstraelen, K. Hemelsoet, A. Van Nieuwenhove, H. J. Ha, M. Waroquier, N. De Kimpe, V. Van Speybroeck, *J. Org. Chem.* **2010**, *75*, 4530–4541; h) B. Dedeoglu, S. Catak, K. N. Houk, V. Aviyente, *ChemCatChem* **2010**, *2*, 1122–1129; i) H. Goossens, K. Vervisch, S. Catak, S. Stankovic, M. D'hooghe, F. De Proft, P. Geerlings, N. De Kimpe, M. Waroquier, V. Van Speybroeck, *J. Org. Chem.* **2011**, *76*, 8698–8709.
[30] a) C. Adamo, M. Cossi, V. Barone, *J. Comput. Chem.* **1997**, *18*, 1993–2000; b) A. Salvà, J. Donoso, J. Frau, F. Muñoz, *J. Phys. Chem. A* **2003**, *107*, 9409–9414; c) A. Salvà, J. Donoso, J. Frau, F. Muñoz, *J. Phys. Chem. A* **2004**, *108*, 11709–11714; d) S. Catak, G. Monard, V. Aviyente, M. F. Ruiz-López, *J. Phys. Chem. A* **2006**, *110*, 8354–8365; e) R. Z. Liao, W. J. Ding, J. G. Yu, W. H. Fang, R. Z. Liu, *J. Phys. Chem. A* **2007**, *111*, 3184–3190; f) S. Catak, G. Monard, V. Aviyente, M. F. Ruiz-López, *J. Phys. Chem. A* **2008**, *112*, 8752–8761; g) S. Catak, G. Monard, V. Aviyente, M. F. Ruiz-López, *J. Phys. Chem. A* **2009**, *113*, 1111–1120; h) S. I. Okovytyy, L. K. Sviatenko, A. A. Gaponov, L. I. Kasyan, I. N. Tarabara, J. Leszczynski, *Eur. J. Org. Chem.* **2010**, 280–291; i) A. T. Durak, H. Gökcan, F. A. S. Konuklar, *Org. Biomol. Chem.* **2011**, *9*, 5162–5171.
[31] N. Agmon, *Chem. Phys. Lett.* **1995**, *244*, 456–462.
[32] A. D. Boese, M. L. M. Jan, *J. Chem. Phys.* **2004**, *121*, 3405–3416.
[33] Y. Zhao, D. G. Truhlar, *J. Phys. Chem. A* **2004**, *108*, 6908–6918.
[34] a) Y. Zhao, D. G. Truhlar, *Theor. Chem. Acc.* **2008**, *120*, 215–241; b) Y. Zhao, D. G. Truhlar, *Acc. Chem. Res.* **2008**, *41*, 157–167.
[35] For recent applications of the M06-2X functional in organic reactions, see: a) L. Liu, D. Malhotra, R. S. Paton, K. N. Houk, G. B. Hammond, *Angew. Chem.* **2010**, *122*, 9318–9321; *Angew. Chem. Int. Ed.* **2010**, *49*, 9132–9135; b) D. Cantillo, C. O. Kappe, *J. Org. Chem.* **2010**, *75*, 8615–8626; c) S. Catak, K. Hemelsoet, L. Hermosilla, M. Waroquier, V. Van Speybroeck, *Chem. Eur. J.* **2011**, *17*, 12027–12036; d) J. M. Winne, S. Catak, M. Waroquier, V. Van Speybroeck, *Angew. Chem.* **2011**, *123*, 12196–12199; *Angew. Chem. Int. Ed.* **2011**, *50*, 11990–11993; e) W. Pluempanupat, M. Abraham, L. Brecker, P.

Wolschann, A. Karpfen, V. B. Arion, M. Wildhalm, *J. Org. Chem.* **2011**, *76*, 3222–3230; f) L. Degennaro, R. Mansueto, E. Carenza, R. Rizzi, S. Florio, L. M. Pratt, R. Luisi, *Chem. Eur. J.* **2011**, *17*, 4992–5003; g) K. Mollet, S. Catak, M. Waroquier, V. Van Speybroeck, M. D′hooghe, N. De Kimpe, *J. Org. Chem.* **2011**, *76*, 8364–8375.

[36] a) A. D. Becke, *J. Chem. Phys.* **1993**, *98*, 5648–5652; b) C. Lee, W. Yang, R. G. Parr, *Phys. Rev. B* **1988**, *37*, 785–789; c) W. J. Hehre, R. Ditchfield, J. A. Pople, *J. Chem. Phys.* **1972**, *56*, 2257–2261; d) R. Krishnan, J. S. Binkley, R. Seeger, J. A. Pople, *J. Chem. Phys.* **1980**, *72*, 650–654.

[37] a) Gaussian 03, Revision C.02, M. J. Frisch, G. W. Trucks, H. B. Schlegel, G. E. Scuseria, M. A. Robb, J. R. Cheeseman, J. A. Montgomery, Jr., T. Vreven, K. N. Kudin, J. C. Burant, J. M. Millam, S. S. Iyengar, J. Tomasi, V. Barone, B. Mennucci, M. Cossi, G. Scalmani, N. Rega, G. A. Petersson, H. Nakatsuji, M. Hada, M. Ehara, K. Toyota, R. Fukuda, J. Hasegawa, M. Ishida, T. Nakajima, Y. Honda, O. Kitao, H. Nakai, M. Klene, X. Li, J. E. Knox, H. P. Hratchian, J. B. Cross, V. Bakken, C. Adamo, J. Jaramillo, R. Gomperts, R. E. Stratmann, O. Yazyev, A. J. Austin, R. Cammi, C. Pomelli, J. W. Ochterski, P. Y. Ayala, K. Morokuma, G. A. Voth, P. Salvador, J. J. Dannenberg, V. G. Zakrzewski, S. Dapprich, A. D. Daniels, M. C. Strain, O. Farkas, D. K. Malick, A. D. Rabuck, K. Raghavachari, J. B. Foresman, J. V. Ortiz, Q. Cui, A. G. Baboul, S. Clifford, J. Cioslowski, B. B. Stefanov, G. Liu, A. Liashenko, P. Piskorz, I. Komaromi, R. L. Martin, D. J. Fox, T. Keith, M. A. Al-Laham, C. Y. Peng, A. Nanayakkara, M. Challacombe, P. M. W. Gill, B. Johnson, W. Chen, M. W. Wong, C. Gonzalez, J. A. Pople, Gaussian, Inc., Wallingford CT, **2004**; b) Gaussian 09, Revision A.1, M. J. Frisch, G. W. Trucks, H. B. Schlegel, G. E. Scuseria, M. A. Robb, J. R. Cheeseman, G. Scalmani, V. Barone, B. Mennucci, G. A. Petersson, H. Nakatsuji, M. Caricato, X. Li, H. P. Hratchian, A. F. Izmaylov, J. Bloino, G. Zheng, J. L. Sonnenberg, M. Hada, M. Ehara, K. Toyota, R. Fukuda, J. Hasegawa, M. Ishida, T. Nakajima, Y. Honda, O. Kitao, H. Nakai, T. Vreven, J. A. Montgomery, Jr., J. E. Peralta, F. Ogliaro, M. Bearpark, J. J. Heyd, E. Brothers, K. N. Kudin, V. N. Staroverov, R. Kobayashi, J. Normand, K. Raghavachari, A. Rendell, J. C. Burant, S. S. Iyengar, J. Tomasi, M. Cossi, N. Rega, J. M. Millam, M. Klene, J. E. Knox, J. B. Cross, V. Bakken, C. Adamo, J. Jaramillo, R. Gomperts, R. E. Stratmann, O. Yazyev, A. J. Austin, R. Cammi, C. Pomelli, J. W. Ochterski, R. L. Martin, K. Morokuma, V. G. Zakrzewski, G. A. Voth, P. Salvador, J. J. Dannenberg, S. Dapprich, A. D. Daniels, Ö. Farkas, J. B. Foresman, J. V. Ortiz, J. Cioslowski, D. J. Fox, Gaussian, Inc., Wallingford CT, **2009**.

[38] a) K. Fukui, *Acc. Chem. Res.* **1981**, *14*, 363–368; b) C E. Dykstra, G. Frenking, K. S. Kim, G. E. Scuseria, *Theory and Applications of Computational Chemistry*, Elsevier, Amsterdam, **2005**, p. 195.

[39] J. Tomasi, B. Mennuci, R. Cammi, *Chem. Rev.* **2005**, *105*, 2999–3093.

[40] a) V. Barone, M. Cossi, *J. Phys. Chem. A* **1998**, *102*, 1995–2001; b) M. Cossi, N. Rega, G. Scalmani, V. Barone, *J. Comput. Chem.* **2003**, *24*, 669–681.

[41] A. K. Rappe, C. J. Casewit, K. S. Colwell, W. A. Goddard, W. M. Skiff, *J. Am. Chem. Soc.* **1992**, *114*, 10024–10035.

[42] a) M. Head-Gordon, J. A. Pople, M. J. Frisch, *Chem. Phys. Lett.* **1988**, *153*, 503–506; b) M. J. Frisch, M. Head-Gordon, J. A. Pople, *Chem. Phys. Lett.* **1990**, *166*, 275–280; c) M. J. Frisch, M. Head-Gordon, J. A. Pople, *Chem. Phys. Lett.* **1990**, *166*, 281–289.

[43] M. Gerenkamp, S. Grimme, *Chem. Phys. Lett.* **2004**, *392*, 229–235.

Received: February 2, 2012
Revised: June 11, 2012
Published online: September 13, 2012

